JOURNAL OF GUIDANCE, CONTROL, AND DYNAMICS
Vol. 23, No. 3, May–June 2000

Dynamics of a Variable-Mass, Flexible-Body System

Arun K. Banerjee*
Lockheed Martin Advanced Technology Center, L9-24/250, Palo Alto, California 94304

A new formulation of the dynamics of a variable-mass, flexible-body system is presented by extending Kane's equations for variable mass particles to flexible bodies characterized by load-dependent stiffness and assumed modes. The method captures the effects of thrust, mass center change, and changes in transverse vibration frequencies due to mass loss and thrust. An order-*n* formulation with prescribed motion of a gimballed nozzle is given for a flexible rocket. Equations for a planar flexible rocket are illustrated and solved numerically. Open-loop simulations with prescribed gimbal motion show that the difference in large motion flight behavior between a rigid-body model and a flexible-body model of a rocket increases as the flexibility increases. Changes in bending frequencies of a flexible rocket due to mass loss and thrust-induced softening are shown.

Introduction

DYNAMICS of systems with variable mass have a long history. The analytical methods include a simplified particle approach giving rise to the classical rocket equations,[1,2] a control volume approach,[3–5] an equivalent force approach,[6] and a constraint relaxation approach.[7] Of these, the control volume approach, based on Reynold's transport theorem in fluid mechanics, is most comprehensive in that it accounts for details of mass-flow effects, but some of the integrals arising in this approach are very difficult to evaluate.[4] Reference 5 has given some tractable analytical evaluations of propellant burn and combustion chamber geometry to shed light on the effects of mass flow on attitude stability. The particle approach does not address mass-flow effects, though it has been shown in Ref. 8 that equations with flow considerations reduce to the equations given by the particle approach under suitable assumptions. The constraint relaxation approach treats mass loss as a relaxation of the constraints that hold a particle in its rest state and for small time discretization steps yields the same results as the particle approach. The equivalent force approach treats the mass-flow effects as a lumped force, and it has been widely used in industry. Flexible-body effects of systems losing mass have been treated in detail only in Ref. 3. Reference 3 derives the nonlinear partial differential equations with time-varying coefficients for the general motion of flexible rockets with internal flow, and although numerical solutions of the general equations were not given, closed-form solutions to the equations for some special cases of rigid-body motion and vibration were provided, showing that normal modes do not exist. Reference 6 considers for a rigid/flexible system mass loss only from the rigid part.

Simulation of a system of flexible bodies with variable mass, described by many time-varying modes, requires computational efficiency considerations. For this, it is desirable to use order-*n* formulations and parallel processing algorithms. The literature dealing with these is quite extensive with Refs. 9–11 being typical samples. For a small number of bodies, as in the case of a flexible rocket with a gimballed engine, order-*n* formulations are shown to be superior to parallel algorithms using n processors[12] and are reported to be highly efficient even in online computations.[13]

The present paper gives a new formulation of the dynamics of a flexible-body system with variable mass. First, Kane's method,[14] adapted to variable-mass particle and rigid-body systems in Ref. 15, is extended to flexible bodies. This is done by requiring that the particles that lose mass are part of a flexible body whose deformation is given by time-varying modes and frequencies. Concomitant errors of premature linearization caused by the use of modes are compensated for with the use of load-dependent geometric stiffness.[16,17] This approach captures effects of thrust, mass center change, and changing vibration characteristics due to thrust and mass loss. It is shown that Kane's method[14] for flexible bodies losing mass reproduces the Newton–Euler equations for such systems available in the literature, besides giving new, vibration equations. Next, a modification of the algorithm of Ref. 10 is made to develop order-*n* equations with prescribed motion of the gimballed nozzle for the flexible rocket. This becomes useful when a gimbal motion time history is available from optimal control theory. The formulation is quite general, and equations with numerical solutions for a planar flexible rocket are given in detail for illustration.

Received 25 August 1998; revision received 10 July 1999; accepted for publication 9 September 1999.

*Consulting Scientist, Dynamics and Controls. Associate Fellow AIAA.

Kane's Equation for a Variable-Mass Flexible Body

Consider a system of particles P_k, $k = 1, \ldots, n$, each losing mass, and let the motion of the system be described by ν generalized speeds.[14] Particle P_k of mass m^k and velocity $\boldsymbol{v}^k$ at time t is subjected to a force $\boldsymbol{F}^k$, and at time $t + \Delta t$ it acquires a velocity $\boldsymbol{v}^k + \boldsymbol{\Delta v}^k$ by ejecting a particle of mass $(-\dot{m}^k \Delta t)$ with a velocity $\boldsymbol{v}_e^k$ relative to P_k. Acceleration of the ejected mass due to the changed velocity being $(\boldsymbol{v}_e^k/\Delta t)$ the force imparted on the ejected particle is

$$\boldsymbol{F}_i^k = (-\dot{m}^k \Delta t)\left(\boldsymbol{v}_e^k \middle| \ \Delta t\right) \tag{1}$$

By reaction $-\boldsymbol{F}_i^k$ acts on the particle that remains in addition to the force $\boldsymbol{F}^k$ and, appealing to Newton's law, one gets the classical equation for a particle losing mass,

$$m^k \frac{\mathrm{d}\boldsymbol{v}^k}{\mathrm{d}t} = \boldsymbol{F}^k + \dot{m}^k \boldsymbol{v}_e^k \tag{2}$$

This derivation, which differs from those based on the conservation of momentum given in many texts, is due to Professor Thomas Kane of Stanford University. Ge and Cheng[15] dot multiplied the terms in Eq. (2) with the partial velocity[14] $\boldsymbol{v}_r^k$ of P_k with respect to the rth generalized speed to form what they called the extended Kane's equation for variable mass systems:

$$F_r + F_r^* + F_r^{**} = 0 \qquad (r = 1, \ldots, n) \tag{3}$$

where, after writing $\mathrm{d}\boldsymbol{v}^k/\mathrm{d}t$ in the left-hand side of Eq. (2) as $\boldsymbol{a}^k$, one defines

$$F_r = \sum_{k=1}^{k=\nu} \boldsymbol{v}_r^k \cdot \boldsymbol{F}^k \tag{4}$$

$$F_r^* = \sum_{k=1}^{k=\nu} \boldsymbol{v}_r^k \cdot (-m^k \boldsymbol{a}^k) \tag{5}$$

$$F_r^{**} = \sum_{k=1}^{k=\nu} \boldsymbol{v}_r^k \cdot \left(\dot{m}^k \boldsymbol{v}_e^k\right) \tag{6}$$

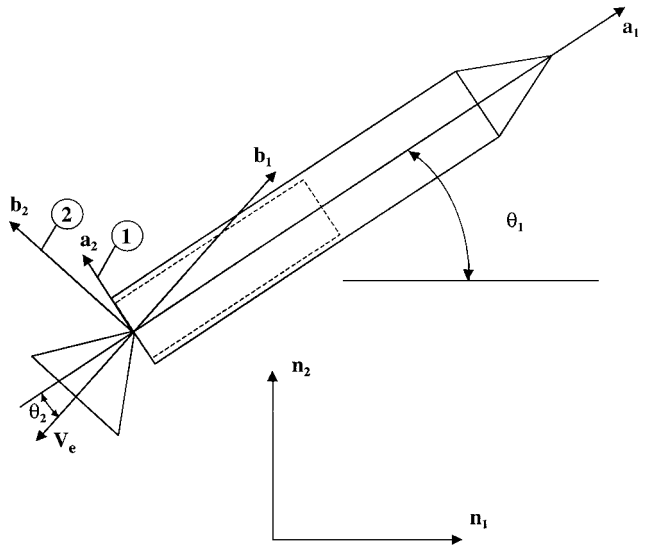

Fig. 1 Planar view of a rocket with a gimballed nozzle.

Extension of these equations to the case when the particles losing mass constitute a flexible body is possible by writing the velocity of an elastically constrained particle in terms of assumed modes and then working with the corresponding partial velocities. Let the small elastic deformations of a generic particle P_k with respect to a reference frame fixed in body 1, the rocket body in Fig. 1, be

$$\boldsymbol{d}^k = \sum_{i=1}^{\mu} \boldsymbol{\phi}_i^k q_i \tag{7}$$

and denote the angular velocity of frame 1 as $\boldsymbol{\omega}^1$, and let the position vector from a fixed point O in frame 1 to P_k be $\boldsymbol{p}^k$. Then the velocity of P_k is

$$\boldsymbol{v}^k = \boldsymbol{v}^O + \boldsymbol{\omega}^1 \times (\boldsymbol{p}^k + \boldsymbol{d}^k) + \sum_{i=1}^{\mu} \boldsymbol{\phi}_i^k \dot{q}_i \tag{8}$$

written in terms of $6 + \mu$ generalized speeds of the body from which follow the expressions for the rth partial velocity of P_k

$$\boldsymbol{v}_r^k = \boldsymbol{v}_r^O + \boldsymbol{\omega}_r^1 \times (\boldsymbol{p}^k + \boldsymbol{d}^k) + \delta_{ri} \boldsymbol{\phi}_i^k \tag{9}$$

where the Kronecker delta associates the rth generalized speed with $\dot{q}_i$. Note in passing that Eq. (8) has been prematurely linearized in the modal coordinates through the small deformation assumption. As has been shown in Refs. 10, 16, and 17, the error in the resulting equations can be compensated for by including geometric stiffness due to resultant loads. The acceleration of P_k is

$$\boldsymbol{a}^k = \boldsymbol{a}^O + \boldsymbol{\alpha}^1 \times (\boldsymbol{p}^k + \boldsymbol{d}^k) + \sum_{i=1}^{\mu} \boldsymbol{\phi}_i^k \ddot{q}_i + \boldsymbol{\omega}^1 \times \left[\boldsymbol{\omega}^1 \times (\boldsymbol{p}^k + \boldsymbol{d}^k) + 2 \sum_{i=1}^{\mu} \boldsymbol{\phi}_i^k \dot{q}_i \right] \tag{10}$$

Kane's equations for a flexible body losing mass can be derived by substituting Eqs. (9) and (10) into Eqs. (4–6). Equations (3) can be separated into translation, rotation, and vibration equations, depending on which of the three terms of the partial velocity equation (9) is non-zero in the dot multiplications of Eqs. (3–6). The translation equations are obtained by dot multiplying with the first term in the right side of Eq. (9):

$$\boldsymbol{v}_r^O \cdot \sum_{k=1}^{\nu} \left\langle m^k \left\{ \boldsymbol{a}^O + \boldsymbol{\alpha}^1 \times (\boldsymbol{p}^k + \boldsymbol{d}^k) + \sum_{i=1}^{\mu} \boldsymbol{\phi}_i^k \ddot{q}_i + \boldsymbol{\omega}^1 \times \left[\boldsymbol{\omega}^1 \times (\boldsymbol{p}^k + \boldsymbol{d}^k) + 2 \sum_{i=1}^{\mu} \boldsymbol{\phi}_i^k \dot{q}_i \right] \right\} - \dot{m}^k \boldsymbol{v}_e^k \right\rangle = \boldsymbol{v}_r^O \cdot \boldsymbol{F}^k \qquad r = 1, 2, 3 \tag{11}$$

These equations agree with those for a system with relative particle motion previously derived in Ref. 2. The term associated with rate of change of mass is identified as due to thrust. The rotation equations follow by dot multiplying Eqs. (3–6) with the second term in the right side of Eq. (9), after using some vector identities representing inertia dyadics:

$$\boldsymbol{\omega}_r^1 \cdot \left\langle \sum_{k=1}^{\nu} (\boldsymbol{p}^k + \boldsymbol{d}^k) \times \left\{ m^k \left[\boldsymbol{a}^O + \sum_{i=1}^{\mu} \boldsymbol{\phi}_i^k \ddot{q}_i \right] - \dot{m}^k \boldsymbol{v}_e^k \right\} + \hat{\boldsymbol{I}} \cdot \boldsymbol{\alpha}^1 + \boldsymbol{\omega}^1 \times \hat{\boldsymbol{I}} \cdot \boldsymbol{\omega}^1 + \sum_{k=1}^{\nu} 2m^k (\boldsymbol{p}^k + \boldsymbol{d}^k) \times \left(\boldsymbol{\omega}^1 \times \sum_{i=1}^{\mu} \boldsymbol{\phi}_i^k \dot{q}_i \right) \right\rangle = \boldsymbol{\omega}_r^1 \cdot \sum_{k=1}^{\nu} (\boldsymbol{p}^k + \boldsymbol{d}^k) \times \boldsymbol{F}^k \qquad r = 4, 5, 6 \tag{12}$$

Equations (12) agree with the basic form of the rotational equation given in Ref. 2, which gives the following more familiar form

$$\boldsymbol{\omega}_r^1 \cdot \left\langle \sum_{k=1}^{\nu} (\boldsymbol{p}^k + \boldsymbol{d}^k) \times \left\{ m^k \left[\boldsymbol{a}^O + \sum_{i=1}^{\mu} \boldsymbol{\phi}_i^k \ddot{q}_i \right] - \dot{m}^k \boldsymbol{v}_e^k \right\} + \frac{\partial^B}{\partial t} (\hat{\boldsymbol{I}} \cdot \boldsymbol{\omega}^1) + \boldsymbol{\omega}^1 \times \left[\sum_{k=1}^{\nu} m^k (\boldsymbol{p}^k + \boldsymbol{d}^k) \times \sum_{i=1}^{\mu} \boldsymbol{\phi}_i^k \dot{q}_i \right] - \sum_{k=1}^{\nu} (\boldsymbol{p}^k + \boldsymbol{d}^k) \times \dot{m}^k [\boldsymbol{\omega}^1 \times (\boldsymbol{p}^k + \boldsymbol{d}^k)] \right\rangle = \boldsymbol{\omega}_r^1 \cdot \sum_{k=1}^{\nu} (\boldsymbol{p}^k + \boldsymbol{d}^k) \times \boldsymbol{F}^k \qquad r = 4, 5, 6 \tag{13}$$

where use has been made of the following identity:

$$\frac{\partial^B}{\partial t} (\hat{\boldsymbol{I}} \cdot \boldsymbol{\omega}^1) = \sum_{k=1}^{\nu} \left\{ \sum_{i=1}^{\mu} m^k \boldsymbol{\phi}_i^k \dot{q}_i \times [\boldsymbol{\omega}^1 \times (\boldsymbol{p}^k + \boldsymbol{d}^k)] + (\boldsymbol{p}^k + \boldsymbol{d}^k) \times \left[\boldsymbol{\omega}^1 \times \sum_{i=1}^{\mu} m^k \boldsymbol{\phi}_i^k \dot{q}_i \right] + (\boldsymbol{p}^k + \boldsymbol{d}^k) \times \dot{m}^k [\boldsymbol{\omega}^1 \times (\boldsymbol{p}^k + \boldsymbol{d}^k)] \right\} + \hat{\boldsymbol{I}} \cdot \boldsymbol{\alpha}^1 + \boldsymbol{\omega}^1 \times \hat{\boldsymbol{I}} \cdot \boldsymbol{\omega}^1 \tag{14}$$

There are two terms involving the rate of change of mass in Eq. (13). Reference 2 labels the first term as the moment due to thrust misalignment and the second one as the moment due to jet damping. Note by referring to Eqs. (13) and (14) that the so-called jet damping term actually vanishes, as it does in Ref. 2. The vibration equations given hereafter account for thrust-induced vibrations and are new, following from Kane's equations by multiplying the third term in Eq. (9) with Eqs. (3–6):

$$\sum_{k=1}^{\nu} \boldsymbol{\phi}_i^k \cdot \left[m^k \left\{ \boldsymbol{a}^O + \boldsymbol{\alpha}^1 \times (\boldsymbol{p}^k + \boldsymbol{d}^k) + \sum_{i=1}^{\mu} \boldsymbol{\phi}_i^k \ddot{q}_i + \boldsymbol{\omega}^1 \times \left[\boldsymbol{\omega}^1 \times (\boldsymbol{p}^k + \boldsymbol{d}^k) + 2 \sum_{i=1}^{\mu} \boldsymbol{\phi}_i^k \dot{q}_i \right] \right\} - \dot{m}^k \boldsymbol{v}_e^k \right] = \sum_{k=1}^{\nu} \boldsymbol{\phi}_i^k \cdot \boldsymbol{F}^k \qquad i = 1, \ldots, \mu \tag{15}$$

Here, to compensate for errors of premature linearization associated with the use of modes,[16] one could consider geometric stiffness arising from the equilibriated system of forces of axial inertia and thrust, as well as aerodynamic forces. Keeping only the thrust effect, one computes the generalized force associated with load-dependent geometric stiffness as

$$S^g = \phi^t K_g \phi f \tag{16}$$

where K_g is the geometric stiffness due to unit thrust and f is the thrust along the axial unit vector,

$$f = \sum_{k=1}^{\nu} \left(\dot{m}^k \boldsymbol{v}_e^k\right) \cdot \boldsymbol{i} \tag{17}$$

and the right-hand side of Eq. (15) becomes

$$\sum_{k=1}^{\nu} \boldsymbol{\varphi}_i^k \cdot \boldsymbol{F}^k = \sum_{j=1}^{\mu} S_{ij}^g q_j - m\left(\omega_i^2 q_i + 2\zeta_i \omega_i \dot{q}_i\right) + \sum_{k=1}^{\nu} \boldsymbol{\varphi}_i^k \cdot \boldsymbol{f}_{\text{ext}}^k$$

$$(i = 1, \ldots, \mu) \tag{18}$$

Mass loss and thrust cause changes in the assumed modes and frequencies. Whereas the frequencies increase with mass loss, the effect of axial thrust is to lower the frequencies.[18] These effects can be considered exactly by repeatedly solving the eigenvalue problem, or approximately by updating the modal frequencies and mode shapes from a table generated for a few frozen configurations.

Before closing this section, it is proper to consider some of the limitations of the particle-based formulation given in this section. The most obvious omission is the consideration of flow of the combustion gases inside the rocket, which gives rise to forces and moments due to the Coriolis effect and unsteady flow. Fortunately, for solid-propellant launch vehicles, these effects are negligible, and even for liquid rockets the only flow can be assumed to be that of the burnt gases being expelled through the nozzle.[19] Reference 20 considers the effects of various assumptions regarding the nature of the exit flowfield (e.g., uniform, parabolic, etc.) on the stability of rocket attitude motion. In terms of the present formulation, one can make, in principle, such assumptions regarding the exit velocity of each combustible particle and, thus, embed the effects of a flowfield.

Matrix Form of the Dynamical Equations

Thus far we have written the equations in vector notation. For the implementation of these in an algorithm, we shall need the scalar equations. To this end, we express all vectors in the basis fixed in the frame for the flexible body, frame 1, and invoke the modal identities of Ref. 19 where the integrals can be replaced by summations over all particles of instantaneous mass m^k and mode ϕ^k. This process results in the translation and rotation equations (11) and (12), becoming

$$M_1 \begin{Bmatrix} a^O \\ \alpha^1 \end{Bmatrix} + A_1^t \ddot{q} + X_1 = \begin{Bmatrix} 0 \\ 0 \end{Bmatrix} \tag{19}$$

where the following notations have been used with U being an identity matrix and where the tilde sign represents the standard skew-symmetric matrix formed out of the elements of the corresponding three-element column matrix:

$$M_1 = \begin{bmatrix} m_1 U & -\tilde{s}_1 \\ \tilde{s}_1 & I_1 \end{bmatrix} \tag{20}$$

$$A_1^t = \begin{Bmatrix} b \\ g \end{Bmatrix} \tag{21}$$

$$X_1 = \begin{Bmatrix} \tilde{\omega}_1(\tilde{\omega}_1 s_1 + 2b\dot{q}) - \dot{m} V_e - f_{\text{ext}}^1 \\ \tilde{\omega}_1 I_1 \omega^1 + 2\sum_{i=1}^{\mu} N_i^t \dot{q}_i \omega^1 - \dot{m} \tilde{r}_c V_e - t_{\text{ext}}^1 \end{Bmatrix} \tag{22}$$

Here use has been made of the following modal integrals[19] that automatically account for the mass center change effect when mass depletion occurs from only a portion of the rocket:

$$b = \sum_{k=1}^{\nu} \phi^k m^k \tag{23}$$

$$g = \sum_{k=1}^{\nu} \tilde{p}^k \phi^k m^k \tag{24}$$

$$s = \sum_{k=1}^{\nu} p^k m^k + bq \tag{25}$$

$$N_i = \sum_{k=1}^{\nu} \left[\left(p^{k^t} \phi_i^k\right) U - p^k \left(\phi_i^k\right)^t\right] m^k \qquad i = 1, \ldots, \mu \tag{26}$$

$$I_1 = I_1^0 + \sum_{i=1}^{\mu} \left(N_i + N_i^t\right) q_i \tag{27}$$

$$\tilde{r}_c = \frac{1}{n} \sum_{k=1}^{n} (\tilde{p}_k + \tilde{d}_k) \tag{28}$$

It is assumed that all particles have the same ejection speed V_e and mass-loss rate. The vibration equations for a flexible body losing mass, Eqs. (14), in matrix form are

$$A_1 \begin{Bmatrix} a^O \\ \alpha^1 \end{Bmatrix} + E_1 \ddot{q} + Z_1 = 0 \tag{29}$$

where the associated matrices are described as follows:

$$E_1 = \sum_{k=1}^{\nu} \phi^{k^t} m^k \phi^k \tag{30}$$

$$Z_1 = Y_1 + (m\Omega^2 + K^g f) q + 2m\zeta\Omega\dot{q} - \phi^t f_{\text{ext}} \tag{31}$$

$$Y_1 = \begin{Bmatrix} -\omega^{1^t}\left(D_1 \omega^1 - 2\sum_{j=1}^{\mu} d_{1j}\dot{q}_j\right) \\ \vdots \\ -\omega^{1^t}\left(D_\mu \omega^1 - 2\sum_{j=1}^{\mu} d_{\mu j}\dot{q}_j\right) \end{Bmatrix} - \dot{m} \sum_{k=1}^{n} \phi_k^t V_e \tag{32}$$

where use is made of the following modal integrals[20]:

$$D_r = N_r + \sum_{k=1}^{\nu} \sum_{i=1}^{\mu} q_i \left[\phi_i^{k^t} \phi_r^k U - \phi_i^k \phi_r^{k^t}\right] m^k \qquad r = 1, \ldots, \mu \tag{33}$$

$$d_{rj} = \sum_{k=1}^{\nu} \tilde{\phi}_r^k \phi_j^k m^k \qquad (r, j = 1, \ldots, \mu) \tag{34}$$

All of the modal integrals in Eqs. (23–26) and (33) and (34) can be approximately computed assuming invariant mode shapes from a finite element code for current values of the mass distribution using the method of Ref. 21.

Order-*n* Algorithm for a Flexible Rocket with Prescribed Nozzle Motion

A flexible-body rocket with a gimballed nozzle may be treated as two articulated bodies, with the flexible body subjected to combustion and associated mass loss and the nozzle modeled as rigid with invariant mass. The flexible rocket is modeled as a set of finite elements with N lumped masses, of which ν of the lumped masses vary with time. The overall system can be modeled with $(8 + \mu)$ generalized speeds that includes six rigid-body degrees of freedom

for the flexible body with μ vibration modes and two relative rotations in pitch and yaw for the gimballed nozzle. Direct use of Kane's equations, Eqs. (19) and (29), gives rise to a time-varying, dense mass matrix of order $(8 + \mu)$, and when μ is large, computations become time consuming. This may not be acceptable in online applications or during design iterations, and an algorithm that gives rise to block-diagonal mass matrices may be desired. When the interaction control torque applied by the nozzle on the rocket is known, the procedure of Ref. 10 can be directly applied, and the algorithm is given without derivation in the Appendix. When the nozzle angle motion time history is prescribed, as for example, from an optimal flight control solution, this algorithm needs to be modified. Whereas a high-bandwidth nozzle gimbal controller can always be designed to realize the prescribed motion, this requires small integration step sizes in simulation. The modification of the order-n algorithm described here allows larger integration steps by exploiting the prescribed motion information. In preparation for this algorithm, we express the necessary kinematical vectors for each body in its own reference frame. Thus, if the velocity of the point O in Fig. 1 in frame 1 is v^O with generalized speeds u_1, u_2, and u_3 the acceleration of O is

$$a^O = \dot{v}^O + \tilde{\omega}^1 v^O \tag{35}$$

With u_4, u_5, and u_6 being the generalized speeds of the angular velocity of frame 1 in its own basis, angular acceleration of frame 1 has components

$$\alpha^1 = [\dot{u}_4 \dot{u}_5 \dot{u}_6]^t \tag{36}$$

The nozzle has its reference frame, frame 2, with a fixed point that coincides with O of the flexible body. Frame 2 is oriented with respect to frame 1 by a body experiencing 2–3 rotations through given time histories of θ_1 and θ_2. Angular velocity of frame 2 is given in its own basis by the matrix relations

$$\omega^{(2)} = C_{12}^t \omega^1 + R \begin{Bmatrix} \dot{\theta}_1 \\ \dot{\theta}_2 \end{Bmatrix} \tag{37}$$

$$R = \begin{bmatrix} \sin\theta_2 & 0 \\ \cos\theta_2 & 0 \\ 0 & 1 \end{bmatrix} \tag{38}$$

The angular acceleration of frame 2 in its basis can be split into terms involving derivatives of the generalized speeds of the rocket body and remainder terms that include prescribed motion,

$$\alpha^{(2)} = \alpha_0^{(2)} + \alpha_t^{(2)} \tag{39}$$

where

$$\alpha_0^{(2)} = C_{12}^t \alpha^1 \tag{40}$$

$$\alpha_t^{(2)} = \left[\dot{R} + C_{12}^t \tilde{\omega}^1 C_{12} R\right] \begin{Bmatrix} \dot{\theta}_1 \\ \dot{\theta}_2 \end{Bmatrix} + R \begin{Bmatrix} \ddot{\theta}_1 \\ \ddot{\theta}_2 \end{Bmatrix} \tag{41}$$

The order-n algorithm for prescribed motion is started by first applying Kane's equation to the dynamics of the nozzle . To this end, we write the resultant of inertia and external forces and torques about O on body 2 in its own basis, including the unknown forces/torques of interaction from body 1.

$$\begin{Bmatrix} f^{*2} - f^{\text{ext2}} \\ t^{*2} - t^{\text{ext2}} \end{Bmatrix} = M_2 \begin{Bmatrix} a^O \\ \alpha^{(2)} \end{Bmatrix} + \begin{Bmatrix} \tilde{\omega}_2 \tilde{\omega}_2 s_2 - f^{\text{ext2}} \\ \tilde{\omega}_2 I_2 \omega_2 - t^{\text{ext2}} \end{Bmatrix} \tag{42}$$

where M_2 is given by Eq. (20) for a rigid body. One can write, in view of Eqs. (39) and (40),

$$\begin{Bmatrix} a^O \\ \alpha^{(2)} \end{Bmatrix} = W \begin{Bmatrix} a^O \\ \alpha^1 \end{Bmatrix} + \begin{Bmatrix} 0 \\ \alpha_t^{(2)} \end{Bmatrix} \tag{43}$$

where W is the matrix made up of the direction cosine matrix relating frame 1 to frame 2,

$$W = \begin{bmatrix} C_{12}^t & 0 \\ 0 & C_{12}^t \end{bmatrix} \tag{44}$$

so that Eq. (42) can be rewritten as

$$\begin{Bmatrix} f^{*2} - f^{\text{ext2}} \\ t^{*2} - t^{\text{ext2}} \end{Bmatrix} = M_2 W \begin{Bmatrix} a^O \\ \alpha^1 \end{Bmatrix} + X_2 \tag{45}$$

where

$$X_2 = M_2 \begin{Bmatrix} 0 \\ \alpha_t^{(2)} \end{Bmatrix} + \begin{Bmatrix} \tilde{\omega}_2 \tilde{\omega}_2 s_2 - f^{\text{ext2}} \\ \tilde{\omega}_2 I_2 \omega_2 - t^{\text{ext2}} \end{Bmatrix} \tag{46}$$

Equation (45) accounts for the inertia and external forces and moments on the nozzle, including unknown interaction forces at O and moments about O applied by the rocket, expressed in the frame-2 basis. It will be necessary later to express these forces and moments in the frame-1 basis. This is done using the transformation matrix of Eq. (44) so that

$$\begin{Bmatrix} f^{*2} - f^{\text{ext2}} \\ t^{*2} - t^{\text{ext2}} \end{Bmatrix} = W^t M_2 W \begin{Bmatrix} a^O \\ \alpha^1 \end{Bmatrix} + W^t X_2 \tag{47}$$

In preparation for considering the inertia forces and torques on the flexible body, body 1, we first write the solution of Eq. (29) symbolically as

$$\ddot{q} = -E_1^{-1} \left(A_1 \begin{Bmatrix} a^O \\ \alpha^1 \end{Bmatrix} + Z_1 \right) \tag{48}$$

where the interaction forces and moments do not appear in the right side by virtue of the assumption that the elastic deformation at the origin of coordinates O is zero. It may be noted here that E_1, given by Eq. (30), is a diagonal matrix for variable mass. Now the system of inertia and external forces and moments on body 1, including interaction forces/torques from body 2, can be expressed in body 1 basis as per Eq. (19).

$$\begin{Bmatrix} f^{*1} - f^{\text{ext1}} \\ t^{*1} - t^{\text{ext1}} \end{Bmatrix} = M_1 \begin{Bmatrix} a^O \\ \alpha^1 \end{Bmatrix} + A_1^t \ddot{q} + X_1 \tag{49}$$

Use of Eq. (48) in Eq. (49) and introduction of the notations

$$\hat{M}_1 = M_1 - A_1^t E_1^{-1} A_1 \tag{50}$$

$$\hat{X}_1 = X_1 - A_1^t E_1^{-1} Z_1 \tag{51}$$

lead to the resultant of all inertia and external forces and torques on body 1 in its basis to be

$$\begin{Bmatrix} f^{*1} - f^{\text{ext1}} \\ t^{*1} - t^{\text{ext1}} \end{Bmatrix} = \hat{M}_1 \begin{Bmatrix} a^O \\ \alpha^{(1)} \end{Bmatrix} + \hat{X}_1 \tag{52}$$

Finally considering the system of the two bodies, the interaction forces and torques between the bodies cancel and the resultant of the inertia and external forces on these two bodies is obtained by summing Eqs. (47) and (52). This system of forces and torques is in dynamic equilibrium. This gives rise to the linear algebraic equation for computing the base acceleration,

$$\left[W^t M_2 W + \hat{M}_1\right] \begin{Bmatrix} a^O \\ \alpha^1 \end{Bmatrix} + \left\{W^t X_2 + \hat{X}_1\right\} = 0 \tag{53}$$

Solution of Eq. (53), for a^O and α^1 leads to the explicit statement of the kinematical differential equations (35) and (36) and the vibration equation (48) of the flexible rocket body. This completes the order-n algorithm with prescribed nozzle rotation.

Numerical Example

The order-n equations for planar motion of a flexible rocket with prescribed motion of the gimballed nozzle are given here. For simplicity the missile body is represented as a beam of length L

cantilevered to the aft motor dome where the nozzle connects to the main body, and is described by two modes. The mode shapes and the modal integrals are functions of the roots λ_i of the cantilever beam characteristic equation as follows:

$$\phi_i(x) = \cosh(\lambda_i x/L) - \cos(\lambda_i x/L) - \sigma_i[\sinh(\lambda_i x/L) - \sin(\lambda_i x/L)] \qquad i = 1, 2 \tag{54}$$

where

$$\sigma_i = \frac{\cosh\lambda_i + \cos\lambda_i}{\sinh\lambda_i + \sin\lambda_i} \qquad i = 1, 2 \tag{55}$$

$$\int_B \phi_i^2 \, \mathrm{d}m = m_1 \qquad i = 1, 2 \tag{56}$$

$$b_{2i} = \int_B \phi_i \, \mathrm{d}m = 2m_1\sigma_i/\lambda_i \qquad i = 1, 2 \tag{57}$$

$$g_i = \int_B x\phi_i \, \mathrm{d}m = 2m_1 L/\lambda_i^2 \qquad i = 1, 2 \tag{58}$$

The matrices A_1, E_1, M_1, and X_1 are given, respectively, from Eqs. (21), (30), (20), and (22) by

$$A_1 = \begin{bmatrix} 0 & b_{21} & g_1 \\ 0 & b_{22} & g_2 \end{bmatrix} \tag{59}$$

$$E_1 = \mathrm{diag}(m_1, m_1) \tag{60}$$

$$M_1 = \begin{bmatrix} m_1 & 0 & -s_2 \\ 0 & m_1 & s_1 \\ -s_2 & s_1 & J_1 \end{bmatrix} \tag{61}$$

$$X_1 = \begin{Bmatrix} -\dot\theta_1^2 s_1 - 2\dot\theta_1 \sum_{i=1}^{2} b_i\dot q_i - \dot m V_e \cos\theta_2 - f_{\mathrm{ext}}^{(1)} \\ -\dot\theta_1^2 s_2 - f_{\mathrm{ext}}^{(2)} - \dot m V_e \sin\theta_2 \\ \dot m V_e\left(\sum_{i=1}^{2}\varphi_i\left(\frac{L}{2}\right)q_i\cos\theta_2 - \frac{L}{2}\sin\theta_2\right) - t_{\mathrm{ext}}^{(1)} \end{Bmatrix} \tag{62}$$

where θ_2 is the prescribed nozzle angle and Eq. (25) defines

$$\begin{Bmatrix} s_1 \\ s_2 \end{Bmatrix} = \begin{Bmatrix} m_1 L/2 \\ b_{21}q_1 + b_{22}q_2 \end{Bmatrix} \tag{63}$$

The two components of the external force and the torque due to aerodynamics and gravity on the rocket body are expressed in the body basis as

$$\begin{Bmatrix} f^{\mathrm{ext1}} \\ t^{\mathrm{ext1}} \end{Bmatrix} = 0.5\rho(\dot x^2 + \dot y^2)A_s \begin{Bmatrix} C_x \\ C_y \\ L_m C_m + 0.0212L\alpha \end{Bmatrix} - m_1 g \begin{Bmatrix} \sin\theta_1 \\ \mathrm{cosn}\,\theta_1 \\ 0.5L\cos\theta_1 \end{Bmatrix} \tag{64}$$

Here A_s is the aerodynamic surface area, L_m is a characteristic length for the aerodynamic moment, and C_x, C_y, and C_m are the aerodynamic coefficients given as functions of the angle of attack α. Matrix Z_1 is given by Eq. (31) as incorporating Eq. (18)

$$Z_1 = \begin{Bmatrix} m_1(\omega_1^2 - \dot\theta_1^2)q_1 \\ m_1(\omega_2^2 - \dot\theta_2^2)q_2 \end{Bmatrix} + \frac{6\dot m V_e}{5L}\begin{Bmatrix} \varphi_1^2(L)q_1 + \varphi_1(L)\varphi_2(L)q_2 \\ \varphi_2^2(L)q_2 + \varphi_1(L)\varphi_2(L)q_1 \end{Bmatrix} - f_{\mathrm{ext}}^{(2)}\begin{Bmatrix} \varphi_1\left(\frac{L}{2}\right) \\ \varphi_2\left(\frac{L}{2}\right) \end{Bmatrix} \tag{65}$$

Here the second column matrix represents the geometric stiffness effect due to thrust on a cantilever beam.[22] For the nozzle oriented as in Fig. 1, matrices M_2 and X_2 follow from Eqs. (20) and (22) for rigid bodies:

$$M_2 = \begin{bmatrix} m_2 & 0 & 0 \\ 0 & m_2 & -m_2 r_2 \\ 0 & -m_2 r_2 & J_2 \end{bmatrix} \tag{66}$$

$$X_2 = \begin{Bmatrix} 0 \\ -m_2 r_2 \\ J_2 \end{Bmatrix}\ddot\theta_2 + \begin{Bmatrix} m_2\left(\dot\theta_1 + \dot\theta_2\right)^2 r_2 + m_2 g\sin(\theta_1 + \theta_2) \\ m_2 g\cos(\theta_1 + \theta_2) \\ -m_2 g r_2\cos(\theta_1 + \theta_2) \end{Bmatrix} \tag{67}$$

The direction cosine matrix of Eq. (44), referring to Fig. 1, becomes

$$W = \begin{bmatrix} \cos\theta_2 & \sin\theta_2 & 0 \\ -\sin\theta_2 & \cos\theta_2 & 0 \\ 0 & 0 & 1 \end{bmatrix} \tag{68}$$

Open-loop control in the form of prescribed motion of the gimballed nozzle is obtained by simplifying an actual time history by the following function:

$$\theta_2 = 2.618 \times 10^{-3} t \qquad t < 10 \tag{69}$$

$$\theta_2 = 2.618 \times 10^{-2}\left[1 - \frac{t-10}{60}\right] + 5.236 \times 10^{-3}\sin\frac{\pi(t-10)}{30} \qquad 10 < t < 70 \tag{70}$$

Now matrices in Eqs. (50) and (51) can be formed. Equation (53) is then set up where

$$\begin{Bmatrix} a^O \\ \alpha^1 \end{Bmatrix} = \begin{Bmatrix} \ddot x_1 - \dot y_1\dot\theta_1 \\ \ddot y_1 + \dot x_1\dot\theta_1 \\ \ddot\theta_1 \end{Bmatrix} \tag{71}$$

written in terms of the body components of velocity, $\dot x_1$ and $\dot y_1$. Finally, the gimbal torque required to realize the prescribed motion can be written by reducing to planar case Eq. (A6) given in the Appendix,

$$\tau_c = -J_2\ddot\theta_2 - [0, -m_2 r_2, J_2]W\begin{Bmatrix} a^O \\ \alpha^1 \end{Bmatrix} + m_2 g r_2\cos(\theta_1 + \theta_2) \tag{72}$$

The equations developed for the example problem were coded by the symbol manipulator program, AUTOLEV.[23] Numerical simulation was carried out for the following data: $m_1 = 4400$ slug, $m_2 = 90$ slug, $L = 60$ ft, $\dot m = -39$ slug/s, $V_e = -I_{\mathrm{sp}}g$, with specific impulse $I_{\mathrm{sp}} = 267$, $J_2 = 200$ slug-ft^2, $r_2 = 0.5$ ft, $Q = 2425$ lb/ft^2,

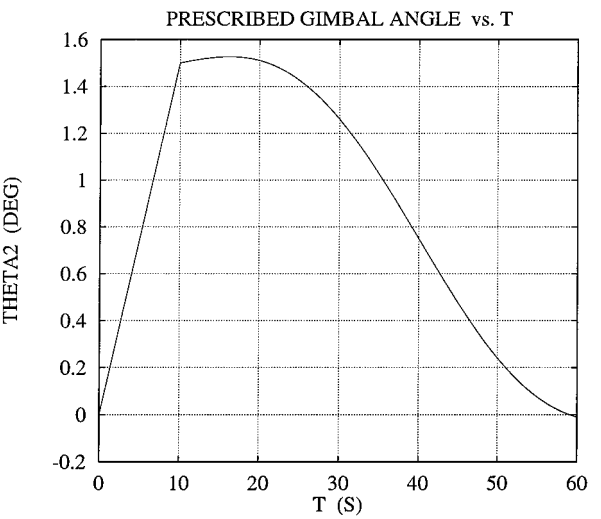

Fig. 2 Prescribed motion time history of the nozzle gimbal angle.

$A_s = 46\ \text{ft}^2$, and $L_m = 21.4$ ft. The cantilever beam with $EI = 1.14 \times 10^9$ lb-ft^2 had initial first two natural frequencies, 1.05 and 6.6 Hz, respectively.

The aerodynamic coefficients were given by $C_x = 0.0115\alpha - 0.420$, $C_y = -0.0425\alpha$, and $C_m = 0.149\alpha$. In computing the dynamic pressure term in Eq. (64), an exponential density model was used with the inertial vertical component of position y_i:

$$\rho = 2.377 \times 10^{-3} \exp(-4.15 \times 10^{-5} y_i) \tag{73}$$

Three simulations were performed with these data: that for a rigid rocket, that for a rocket with low flexibility (36 times the value of EI given earlier), and that for high flexibility. The rigid-body response equations were obtained by zeroing out all terms having to do with flexibility in the basic formulation given in the paper.

Figure 2 is the input to the codes of prescribed motion of the nozzle angle with respect to the rocket, as defined by Eqs. (69) and (70). Figure 3 has three plots of the height of the rocket from the ground, for low- and high-flexibility models, and for the rigid-body model of the rocket, and results show the difference that flexibility makes. There is a noticeable difference for the high-flexibility result from the rigid or low-flexibility result. Figure 4 shows the inertial horizontal displacement vs time of the rocket for the two flexible models and the rigid model. Although the difference between the rigid and low-flexibility models is small, there is a significant difference between these and the high-flexibility model. The difference between the rigid and the flexible rocket models is further shown in pitch angle response in Fig. 5, with the difference increasing as the body becomes more flexible. An implication for control implementation from the results in Fig. 5 is that a gyro placed on a flexible rocket would read differently from that on a rigid rocket; this difference also depends on location of the gyro along the rocket. How bending deformations vary along the length of the rocket is illustrated in Fig. 6, which shows the deflections at the midpoint and the tip of the highly flexible rocket. Note that the deflection is negative

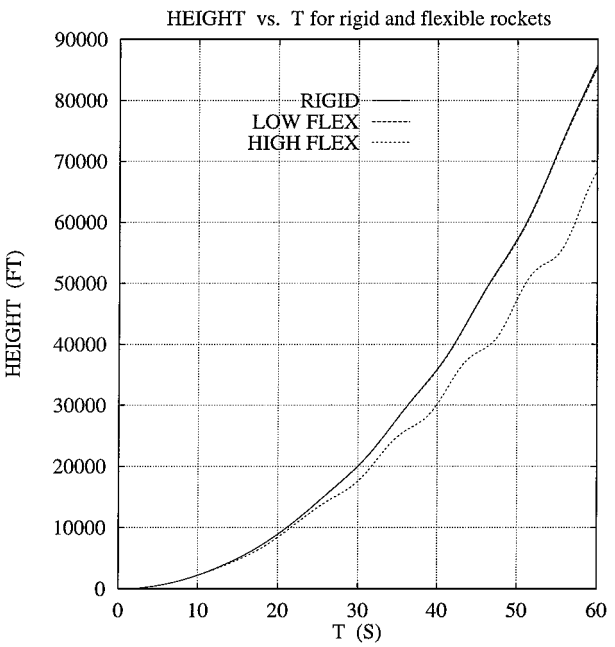

Fig. 3 Height of the rocket from the ground vs time, given by three rocket models.

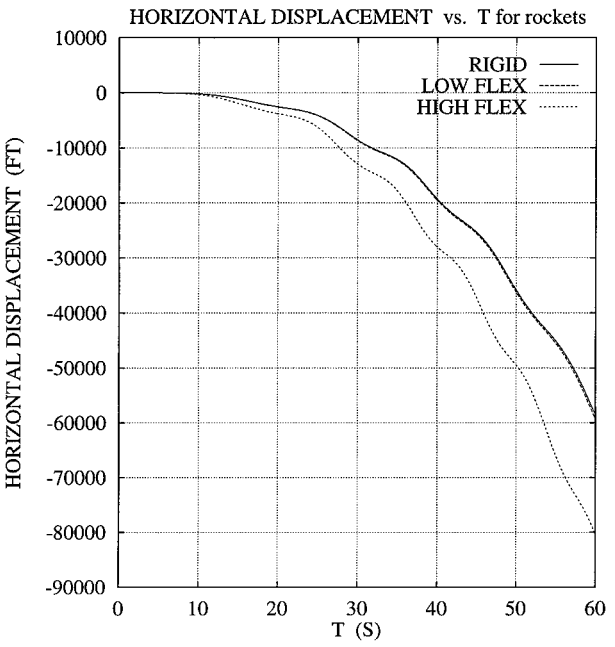

Fig. 4 Horizontal displacement of the rocket vs time, given by three rocket models.

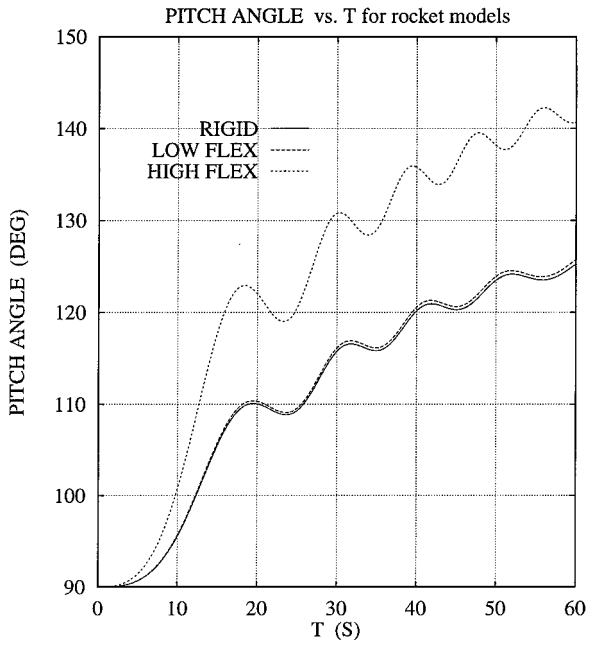

Fig. 5 Pitch angle of the rocket vs time, given by three rocket models.

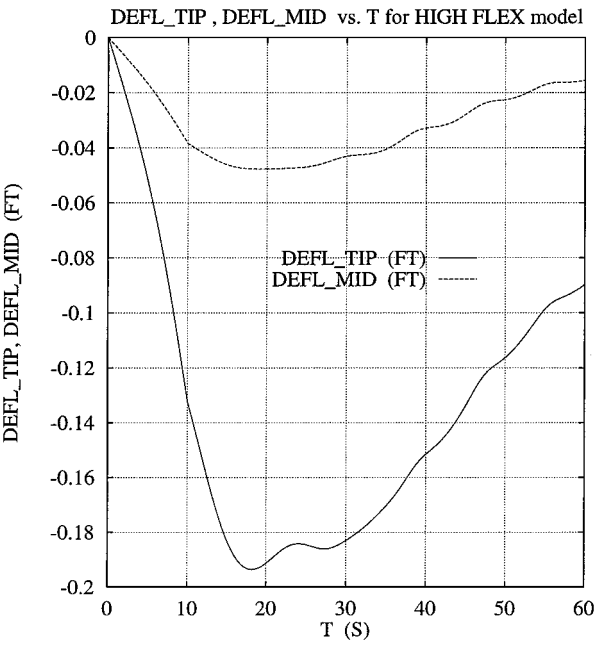

Fig. 6 Tip and midpoint deflection of the high-flexibility rocket model vs time.

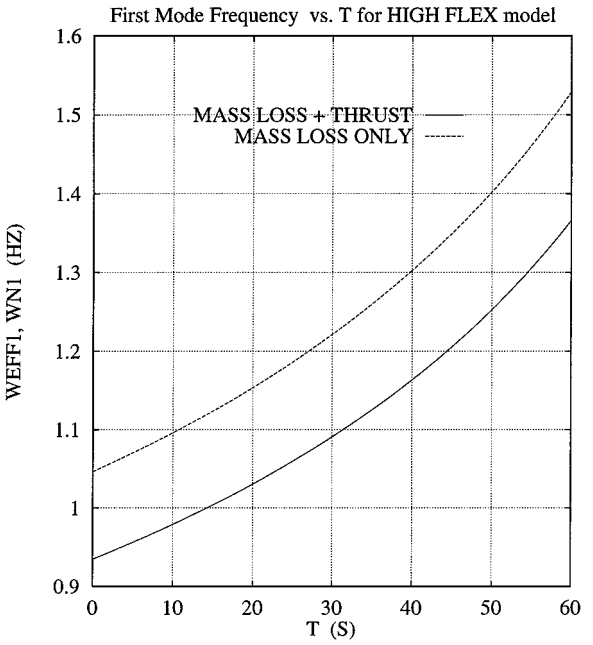

Fig. 7 First mode frquency of high-flexibility rocket model vs time with mass loss only (dotted line) and under the combined action of mass loss and thrust.

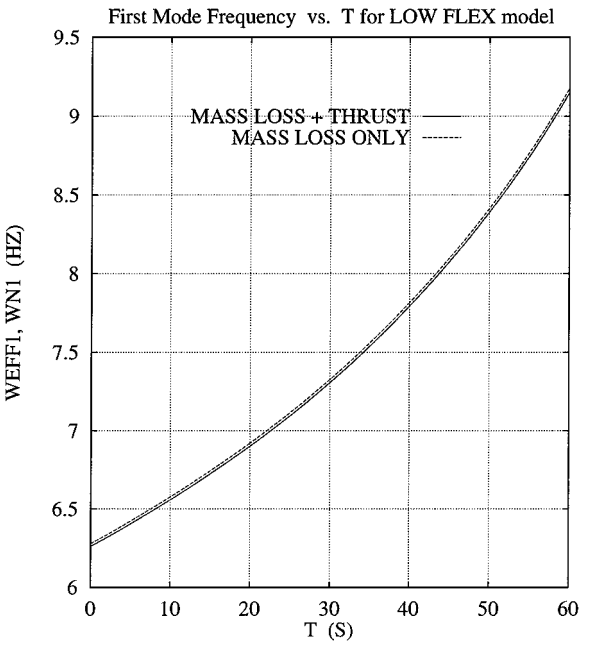

Fig. 8 First mode frquency of low-flexibility rocket model vs time with mass loss only (dotted line) and under the combined action of mass loss and thrust.

corresponding to a positive nozzle angle, which gives a positive transverse component of the thrust; this means that the bending deflection is due to the inertia forces resulting from the transverse component of the thrust. Figure 7 shows the natural and effective first-mode frequency of the highly flexible rocket, with the dashed curve showing the rise in natural frequency with time, indicating mass-loss effect without any thrust; the solid curve shows the actual or effective frequency variation with time, when both mass loss and thrust are considered. The softening action of the system of compressive forces made up of thrust and inertia is apparent from Fig. 7. Figure 8 shows the natural and effective frequencies corresponding to the first mode of vibration for the low-flexibility model vs time due. Figure 9 shows the time history of the gimbal torque needed to realize the prescribed gimbal motion for the high-flexibility model.

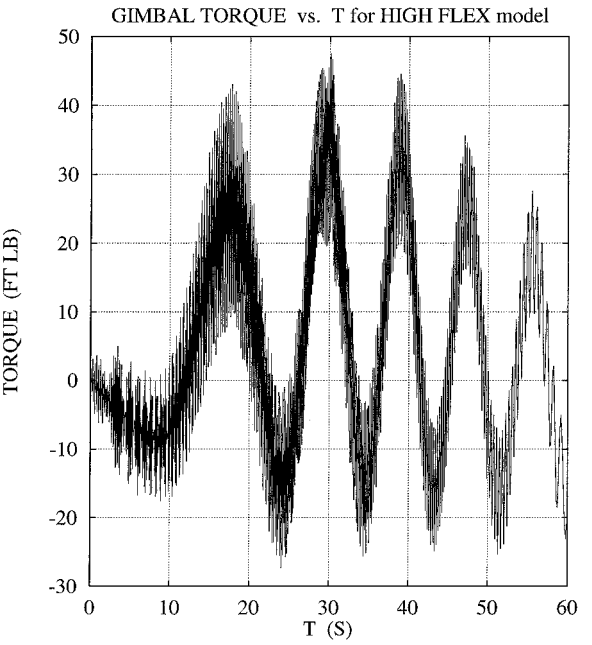

Fig. 9 Gimbal torque in the high-flexibility rocket simulation with specified gimbal motion vs time.

Conclusions

A theory of flexible rocket dynamics suitable for real-time computation is developed in the form of Kane's equations for a flexible body losing mass. The method captures the effects of thrust, mass center change, and change in transverse vibration frequencies due to mass loss and thrust. An order-n version of the equations of motion of a rocket with prescribed motion of its nozzle is given. Open-loop control simulations prescribing the gimbal angle motion show that the difference in flight behavior between a rigid-body model and a flexible-body model of a rocket increases as the flexibility of the rocket increases. This highlights the need in flight control simulations of lightweight, slender rockets for having a flexible-body model that accounts for mass loss. It is hoped that the theory presented in this paper will fulfill such a need.

Appendix: Regular Order-n Algorithm

A reduction of the order-n algorithm of Ref. 10 for the simulation of a flexible rocket controlled by gimbal torques τ_1 and τ_2 driving the respective gimbal degrees of freedom θ_1 and θ_2 is given hereafter.

1) Compute M_1, X_1, A_1, M_2, and X_2, as before.

2) Introduce in terms of Eq. (38) the (6×2) partial angular velocity matrix,

$$\Pi = \begin{bmatrix} 0 \\ R \end{bmatrix} \tag{A1}$$

and define for the inertia matrix I_2 of the gimbal

$$\mu = R^t I_2 R \tag{A2}$$

3) Compute for a 6×6 identity matrix U

$$M = \left[U - M_2 \Pi \mu^{-1} \Pi^t\right] M_2 \tag{A3}$$

$$X = \left[U - M_2 \Pi \mu^{-1} \Pi^t\right] X_2 - M_2 \Pi \mu^{-1} \begin{Bmatrix} \tau_1 \\ \tau_2 \end{Bmatrix} \tag{A4}$$

4) Solve the linear algebraic equations, replacing Eq. (54)

$$\left[W^t M W + \hat{M}_1\right] \begin{Bmatrix} a^O \\ \alpha^1 \end{Bmatrix} + \left\{W^t X + \hat{X}_1\right\} = 0 \tag{A5}$$

5) The gimbal dynamics equations are

$$\begin{Bmatrix} \ddot{\theta}_1 \\ \ddot{\theta}_2 \end{Bmatrix} = -\mu^{-1} \left[\Pi^t \left\{M_2 W \begin{Bmatrix} a^O \\ \alpha^1 \end{Bmatrix} + X_2\right\} - \begin{Bmatrix} \tau_1 \\ \tau_2 \end{Bmatrix}\right] \tag{A6}$$

6) The rocket vibration equations are given as before by Eq. (48).

Acknowledgment

It is a pleasure to thank my colleagues, David Levinson, Andrew Imbrie, and Ching-Ju Chang for their help. The computations given in this paper would not have been possible without the help of David Levinson who showed me how to use AUTOLEV to generate a computer code for solving the differential equations derived here. The data used in the example were kindly provided by Andrew Imbrie, and Ching-Ju Chang got me started on the work.

References

[1]Rosser, J. B., Newton, R. R., and Cross, G. L., *Mathematical Theory of Rocket Flight*, McGraw–Hill, New York, 1947, pp. 1–50.

[2]Thomson, W. T., *Introduction to Space Dynamics*, Wiley, New York, 1963, pp. 230–236.

[3]Meirovitch, L., "General Motion of a Variable Mass Flexible Rocket with Internal Flow," *Journal of Spacecraft and Rockets*, Vol. 7, No. 2, 1970, pp. 186–195.

[4]Eke, F. O., and Wang, S.-M., "Equations of Motion of Two-Phase Variable Mass Systems with Solid Base," *Journal of Applied Mechanics*, Dec. 1994, pp. 855–860.

[5]Mao, T.-C., "Attitude Motions of Space-Based Variable Mass Systems," Ph.D. Thesis, Mechanical Engineering Dept., Univ. of California at Davis, Davis, CA, Sept. 1996.

[6]Greensite, A. L., *Analysis and Design of Space Vehicles Flight Control Systems*, Spartan, New York, 1970, pp. 194–259.

[7]Djerassi, S., "An Algorithm for Simulation of Motions of Variable-Mass Systems," *Journal of Guidance, Control, and Dynamics*, Vol. 21, No. 3, 1998, pp. 427–434..

[8]Kane, T. R., "Variable Mass Dynamics ?," *Bulletin of Mechanical Engineering Education*, Vol. 2, No. 20, 1961, pp. 62–65.

[9]Jain, A., and Rodriguez, G., "Recursive Flexible Multibody System Dynamics Using Spatial Operators," *Journal of Guidance, Control, and Dynamics*, Vol. 15, No. 6, 1992, pp. 1453–1466.

[10]Banerjee, A. K., "Block-Diagonal Equations for Multibody Elastodynamics with Geometric Stiffness and Constraints," *Journal of Guidance, Control, and Dynamics*, Vol. 16, No. 6, 1993, pp. 1092–1100.

[11]Pradhan, S., Modi, V. J., and Misra, A. K., "Order-*N* Formulation for Flexible Multibody Systems in Tree Topology: Lagrangian Approach," *Journal of Guidance, Control, and Dynamics*, Vol. 20, No. 4, 1997, pp. 665–672.

[12]Fijany, A., Sharf, I., and D'Eleuterio, G. M. T., "Parallel O(log N) Algorithms for Computation of Manipulator Forward Dynamics," *IEEE Transactions on Robotics and Automation*, June 1995, pp. 389– 400.

[13]Jain, A., and Man, G., "Real-Time Simulation of the Cassini Spacecraft Using DARTS: Functional Capabilities and the Spatial Algebra Algorithm," 5th Annual Conf. on Aerospace Computational Control, Aug. 1992.

[14]Kane, T. R., and Levinson, D. A., *Dynamics, Theory and Applications*, McGraw–Hill, New York, 1983, pp. 40–50.

[15]Ge, Z. M., and Cheng, Y. H., "Extended Kane's Equations for Nonholonomic Variable Mass System," *Journal of Applied Mechanics*, June 1982, pp. 429–431.

[16]Banerjee, A. K., and Dickens, J. M., "Dynamics of an Arbitrary Flexible Body in Large Rotation and Translation," *Journal of Guidance, Control, and Dynamics*, Vol. 13, No. 2, 1990, pp. 221–227.

[17]Wallrapp, O., and Schwertassek, R., "Representation of Geometric Stiffening in Multibody System Simulation," *International Journal for Numerical Methods in Engineering*, Vol. 32, No. 8, 1991, pp. 1833–1850.

[18]Joshi, A., "Free Vibration Characteristics of Variable Mass Rockets Having Large Axial Thrust/Acceleration," *Journal of Sound and Vibration*, Vol. 187, No. 4, 1995, pp. 727–736.

[19]Meirovitch, L., *Methods of Analytical Dynamics*, McGraw–Hill, New York, pp. 483–491.

[20]Wang, S.-M., "Attitude Dynamics of Variable Mass Systems," Ph.D. Thesis, Mechanical Engineering Dept., Univ. of California at Davis, Davis, CA, 1993.

[21]Banerjee, A. K., and Lemak, M. E., "Multi-Flexible Body Dynamics Capturing Motion-Induced Stiffness," *Journal of Applied Mechanics*, Sept. 1991, pp. 766–775.

[22]Storch, J. A., "Modal Integral Evaluation for Flexible Multibody Systems," AIAA Paper 98-4443, Aug. 1998.

[23]Przemieniecki, J. S., *Theory of Matrix Structural Analysis*, McGraw–Hill, New York, 1968, pp. 388–391.